An SVD-Based Approach for Ghost Detection and Removal in High Dynamic Range Images

Abhilash Srikantha, Désiré Sidibé, Fabrice Mériaudeau
Université de Bourgone, Le2i, UMR CNRS 6306, 12 rue de la fonderie, 71200 Le Creusot, France

Abstract

In this paper, we propose a simple method for the ghost detection problem in the context of merging multiple low dynamic range (LDR) images to form a high dynamic range (HDR) image. We show that the second biggest singular values extracted over local spatio-temporal neighbourhoods can be effectively used for ghost region detection. Furthermore, we combine the proposed method with an exposure fusion technique to generate final HDR image free of ghosting artefacts. We present experimental results to illustrate the efficiency of the proposed method and quantitative comparison with other existing approaches show the good performance of our method in detecting and removing ghosting artefacts.

1 Introduction

With a steady rise in the applications of HDR imaging such as in automotive and entertainment industries, there is a need to employ conventional LDR digital cameras to generate HDR images. A classic technique to bridge this gap is to fuse the well exposed regions of many LDR images each of which captures the same physical scene but with varying exposure times.

The multiple exposures fusion technique introduced in [1] has been widely used for HDR image generation due to its simplicity and efficiency [8]. However, the main limitation of this technique is the requirement of a completely static scene while capturing the sequence of LDR images, which is hardly a practical scenario. Indeed, entities that are affected by motion within the LDR sequence manifest themselves as artefacts in the combined HDR image. This problem is termed as the ghosting problem and the artefacts are called ghosts.

In this paper, we propose a method to tackle the ghosting problem using singular value decomposition (SVD). The method is based on extracting local spatio-temporal neighbourhoods and using the second biggest singular value of the matrix formed by pixel values within the neighbourhoods as a measure for ghost detection. The paper is organised as follows. We begin with a brief overview of the related work in section 2. Section 3 presents the proposed method and section 4 shows experimental results and comparison with other approaches. Finally, the paper ends with the conclusions in section 5.

2 Related Methods

Different approaches have been proposed to detect and remove ghosting artefacts in HDR images. Methods such as [9, 3] impose temporal constraints on pixel values across exposures. In other words, they impose the condition that a pixel must only get brighter when exposure time increases. On the other hand, methods such as [7, 6] impose spatial constraints that relate the intensity of a any pixel with the median intensity of that exposure. As this relation must hold irrespective of the exposure time, deviant pixels are classified as ghosts. These methods are robust, fast and work with either small or large sets of input images. However, the limitation of such methods is that they assume each LDR image to be only slightly dominated by ghosts.

Other methods such as [8, 5] exploit the fact that as each LDR image represents the same physical scene, the radiance maps generated by each of them must be the same. Therefore, locations in radiance maps that exhibit high variance are classified as ghost pixels. As such methods work in the radiance domain, they are sensitive to an accurate estimation of the camera response function (CRF). The estimation of the CRF not only adds computational load but also introduces inaccuracies in the obtained ghosts map.

The method in [4] uses joint probability maps to detect low probability intensity transitions and classifies them as ghosts. The method shows very good ghost detection accuracy. Another method presented in [2] employs the linear relation between two corresponding patches in different exposures in the logarithmic do-

main. It then uses RANSAC to perform a best line fit and outlier pixels are classified as ghosts. Such methods are highly sensitive to manually set thresholds that severely affects its robustness and sensitivity to ghosts.

For an overview of recent methods for ghost detection and removal, the reader is referred to [10].

3 Proposed Method

Let $\{L_k\}_{k=1\ldots N}$ be a set of N LDR images arranged in increasing order of exposure times $\{\Delta t_k\}_{k=1\ldots N}$. In the proposed ghost detection method, we exploit the fact that the brightness values of a pixel in two different exposures are linearly dependent. To see why this is the case, we start with the relation between the pixel brightness value and the scene radiance value given by the following equation:

$$E_{uv}^k = \frac{f^{-1}\left(Z_{uv}^k\right)}{\Delta t_k}, \tag{1}$$

where E_{uv}^k and Z_{uv}^k are, respectively, the radiance and pixel values at location (u, v) in exposure L_k, and $f()$ is the camera response function (CRF) that maps the radiance values of the scene to the pixel values in the captured image.

For a digital camera, the radiance values correspond to the physical quantity of light incident on each element of the sensor array. Hence, if the scene is static, the radiance values in different exposures must ideally be the same for any pixel location (u, v), i.e. $E_{uv}^k = E_{uv}^l$ for two different exposures I_k and I_l. Using equation 1, we obtain:

$$f^{-1}(Z_{uv}^k) = \alpha_{kl} f^{-1}(Z_{uv}^l), \tag{2}$$

where $\alpha_{kl} = \Delta t_k / \Delta t_l$ is the ratio of the exposure times.

The above relation assumes the knowledge of the ideal CRF which is often estimated from the given LDR images. The CRF estimation is prone to error and the resulting function although monotonic and regularized, shows local non-linearities. Therefore, to avoid the CRF estimation and process pixel intensities directly, we make two assumptions. We first assume that the CRF is piecewise linear, which means we can assume the pixel values in P consecutive exposures to be linearly related, P being a small number (we use $P = 3$ in our experiments). This first assumption preserves temporal linearity. The second assumption preserves spatial smoothness, i.e. we assume similar pixel values over a local spatial neighbourhood. Of course, local regions with edges are exceptions to this assumption, but this information can be easily incorporated. The experimental results in section 4 show that these assumptions are valid in practice.

Based on the above two assumptions, we define a spatio-temporal neighbourhood for every pixel at spatial location (u, v) by:

$$N_{uv}^{p:q} = \{Z_{u'v'}^k | \Psi_{(u,v),(u',v')} \leq d, k = p, \ldots, q\}, \tag{3}$$

where $Z_{u'v'}^k$ is the pixel intensity value at location (u', v') in exposure L_k, Ψ is the city block distance between the pair of locations (u, v) and (u', v'), d is a value that defines the size of the spatial neighbourhood in each LDR image, and p and q indicate the set of consecutive exposures defining the temporal length of the neighbourhood.

We can rearrange $N_{uv}^{p:q}$ and write it as a matrix $M_{uv}^{p:q}$ containing N rows, the kth row corresponding to the spatial window in exposure L_k represented as a vector of length $Q = d \times d$:

$$M_{uv}^{p:q} = \begin{bmatrix} Z_{u_1v_1}^1 & Z_{u_2v_2}^1 & \cdots & Z_{u_Qv_Q}^1 \\ \vdots & \vdots & \vdots & \vdots \\ Z_{u_1v_1}^N & Z_{u_2v_2}^N & \cdots & Z_{u_Qv_Q}^N \end{bmatrix}. \tag{4}$$

Observing the matrix $M_{uv}^{p:q}$, we see that each of its columns shows the brightness values of a single pixel in different exposures. Based on the two assumptions, these values are linearly related to each other. In other words, all rows of $M_{uv}^{p:q}$ are linearly dependent and the matrix must have rank one. Since the rank of a matrix is equal to the number of non-zero singular values, a rank one matrix has a single non-zero singular value. Therefore, the second biggest singular value of the matrix $M_{uv}^{p:q}$ is an indicator of the the deviation from the linearity assumption and can be used for ghost detection.

3.1 Ghost detection

Given a sequence of N LDR images, we process all sets of P consecutive exposures to generate differents ghost maps separately and finally combine them to get the final ghost map. More precisely, given a set of P consecutive exposures: $\{L_l, L_{l+1}, \cdots, L_{l+P}\}$, we construct the matrix $M_{uv}^{l:l+P}$ as in equation 4, for each spatial location (u, v) and find its singular values using SVD.

For ghost-free areas, the second biggest singular value of the matrix should be small, ideally equal to zero, while for ghost areas this value should be large. Hence, the second biggest singular value can be used to obtain a ghost map for each set of P consecutive exposures. Finally, all those ghost maps are combined into a

final ghost map. Note that to preserve temporal linearity, P should be small.

3.2 Ghost removal

Many methods in literature solve the ghost problem based on the detected ghost map. A common approach consist in combining the different exposures in ghost-free regions while selecting a single reference exposure for ghost areas [8, 5]. Such single exposure selection method can be employed with the proposed method using the detected ghost map in section 3.1. However, the SVD methodology can be employed to generate a ghost-free HDR image.

Using SVD, the matrix $M_{uv}^{p:q}$ can be written as a weighted sum of rank one matrices: $M_{uv}^{p:q} = \sum_{i=1}^{m} \sigma_i u_i v_i^T$, where u_i and v_i are the left and right singular vectors respectively, and the σ_is are the singular values in descending order of magnitude.

Assuming that the moving objects in the scene appear in a small number of exposures at each pixel location, which is a fair and commonly used assumption, the first term of the decomposition, $\sigma_1 u_1 v_1^T$, captures the static part of the scene while the remaining terms correspond to the moving parts. Therefore, we can reconstruct a ghost-free HDR image from the SVD of $M_{uv}^{p:q}$, keeping the first term of the decomposition.

4 Experiments

We perform several experiments to evaluate the performance of the proposed method, both qualitatively and quantitatively. For quantitative evaluation of the ghost detection method, we use the *Office* sequence of images provided in [10]. The sequence is composed of seven exposures with moving objects in the scene, and is designed to test ghost detection on various aspects such as the capability of the method in detecting small ghost regions and the ability of detecting low contrast ghosts. Additionally, the varying frequencies with which the ghosts occur at any given location test the sensitivity of the ghost detection algorithms.

The sequence of exposures and the resulting HDR image with ghosting artefacts are shown in figure 1(a) and (b) respectively. Note the highly pronounced ghosting artefacts caused by the container and the knife at the bottom left and the right locations and the less pronounced ghosts caused by the same moving objects at the central location of the image in figure 1(b). The manually segmented ghost map is shown in figure 1(c) and serves as ground truth.

As explained in section 3.1, several ghost maps are detected for each set of P consecutive exposures and are

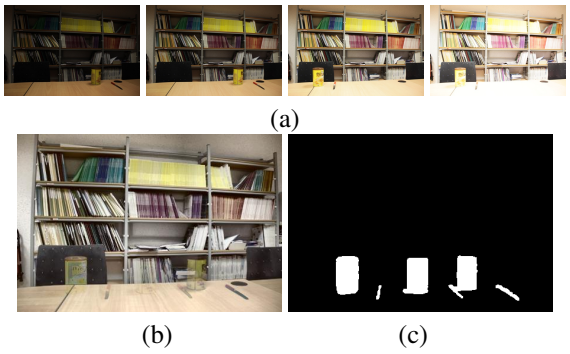

Figure 1. The *Office* sequence. (a) Five of the seven exposures used for ghost detection. (b) HDR image generated showing ghosting artefacts; (c) Manually segmented ground truth ghost map.

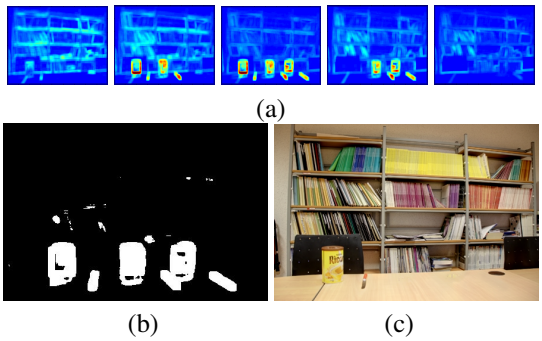

Figure 2. Ghost detection results. (a) Obtained ghost maps for every consecutive 3 images; (b) The final ghost map; (c) The obtained ghost free HDR image.

finally combined into a global ghost map. The number P should be small to satisfy the first assumption, i.e. the linear dependence of pixel values over time. Therefore, we use $P = 3$ in our experiments and set the size of the spatial window to $d = 3$ in each exposure. For the *Office* sequence which contains seven images, we obtain five ghost maps which are fused into a global ghost map. The latter is obtained as the sum of the thresholded individual ghost maps. For each ghost map, we calculate the cumulative histogram of the second singular values and set the threshold such as the top 25% percentile pixels are classified as ghost. The five ghost maps obtained by our SVD based approach are shown in figure 2(a), and the final ghost map is given in figure 2(b). As can be seen, the proposed method performs extremely well and generates very few false positives.

In their review paper [10], the authors compare different state of the art techniques and show that the

Table 1. Comparison of different ghost detection methods using the *Office* sequence in figure 1(a).

Method	Sensitivity	Specificity
Pixel Order [9]	0.617	0.930
Bitmap [7]	0.664	0.807
Prediction [3]	0.678	0.861
Graph-cuts [4]	0.913	0.845
Proposed	**0.927**	**0.965**

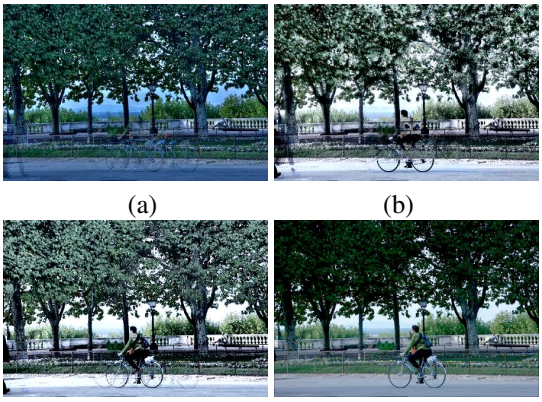

Figure 3. Ghost removal results. (a) HDR image showing ghost artefacts. (b),(c) and (d) Ghost removal results with the methods in [5], [7] and the proposed one, respectively.

best methods, in terms of sensitivity and specificity, for ghost detection are the graph-cuts based method [4], the prediction based method [3], the pixel order method [9] and the bitmap based method [7] respectively. We also compare our method against those approaches and the results are summarized in table 1. It is to be noted that the proposed method performs better than state of the art methods since it shows higher sensitivity and specificity values, i.e. it correctly detects almost all ghost pixels with very few false positives.

The ghost free HDR image obtained by the proposed method with the *Office* sequence is shown in figure 2(c). The method correctly removes all ghosting artefacts and keeps the moving objects at fixed locations. Other ghost removal examples are given in figure 3. For this difficult sequence, the proposed SVD based method gives satisfactory results while the methods in [5, 7], which select a single reference exposure in ghost areas, fail to correctly remove ghosting artefacts caused by the moving cyclist.

5 Conclusion

In this paper, a ghost detection and removal method is proposed for ghost free HDR image generation. The method is based on extracting local spatio-temporal neighbourhoods and uses singular value decomposition of the matrix formed by pixel values within the neighbourhoods to find and remove ghost artefacts. The method is simple and effective as shown by various experiments with different exposure sequences. Comparison with state of the art methods show that the proposed method achieves the best detection results. In particular, it accurately detects almost all ghost pixels with very few false positives, hence leading to a final HDR image free of ghost artefacts.

References

[1] P. Debevec and J. Malik. Recovering High Dynamic Range Radiance Maps from Photographs. In *Proceedings of the SIGGRAPH 97 Conference*, pages 369–378, 1997.

[2] O. Gallo, N. Gelfand, W.-C. Chen, M. Tico, and P. K. Artifact-free High Dynamic Range Imagin. In *Proceedings of the IEEE International Conference on Computational Photography (ICCP)*, pages 1–7, 2009.

[3] T. Grosch. Fast and Robust High Dynamic Range Image Generation with Camera and Object Movement. In *Proceedings of Vision, Modeling and Visualization Conference*, pages 277–284, 2006.

[4] Y.-S. Heo, K.-M. Lee, S.-U. Lee, Y. Moon, and J. Cha. Ghost-free High Dynamic Range Imaging. In *Proceedings of the 10th Asian conference on Computer vision - ACCV*, pages 486–500, 2010.

[5] K. Jacobs, C. Loscos, and W. G. Automatic High Dynamic Range Image Generation of Dynamic Environments. *IEEE Computer Graphics and Applications*, 28(2):84–93, 2008.

[6] T.-H. Min, R.-H. Park, and S.-K. Chang. Histogram Based Ghost Removal in High Dynamic Range Images. In *Proceedings of the International Conference on Multimedia and Expo - ICME*, pages 530–533, 2009.

[7] F. Pece and J. Kautz. Bitmap Movement Detection: HDR for Dynamic Scenes. In *Proceedings of Visual Media Production (CVMP)*, pages 1–8, 2010.

[8] E. Reinhard, G. Ward, S. Pattanaik, and P. Debevec. *High Dynamic Range Imaging: Acquisition, Display and Image-Based Lighting*. Morgan Kauffman, 2005.

[9] D. Sidibe, W. Puech, and O. Strauss. Ghost Detection and Removal in High Dynamic Range Images. In *Proceedings of the 17th European Signal Processing Conference - EUSIPCO*, pages 2240–2244, 2009.

[10] A. Srikantha and D. Sidibé. Ghost Detection and Removal for High Dynamic Range Images: Recent Advances. *Signal Processing:Image Communication*, 27(6):650–662, 2012.